TECH NOTE

Tuning Enzymatic Fragmentation with Twist TrueAmp Library Preparation Kit to Control Insert Size and Optimize Sequencing Performance

INTRODUCTION

DNA fragmentation is a critical step in next-generation sequencing (NGS) library preparation, directly influencing insert size distribution, sequencing efficiency, and downstream coverage uniformity. Mechanical shearing methods, such as sonication, are commonly used to generate fragments within a desired size range. While effective, these approaches can introduce DNA damage, require specialized instrumentation, and may limit scalability.

Enzymatic fragmentation offers an alternative approach, enabling controlled DNA fragmentation through nuclease activity. The Twist TrueAmp Library Preparation Kit integrates enzymatic fragmentation with end-repair and dA-tailing into a streamlined workflow, allowing fragment size distributions to be tuned through adjustment of reaction parameters such as temperature and incubation time.

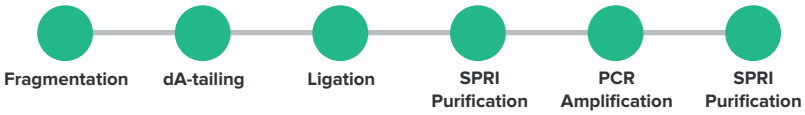

However, suboptimal fragmentation can result in broad insert size distributions, reduced library yield, and biases in sequencing performance. In this technical note, we systematically evaluate how fragmentation conditions within the Twist TrueAmp Library Preparation Kit's workflow influence insert size, library yield, and sequencing outcomes. We further assess the role of SPRI bead-based size selection at key workflow stages to refine library size distributions and improve consistency.

We examine downstream sequencing effects using shallow whole genome sequencing (WGS) on the NextSeq 550 platform. Finally, we evaluate the impact of DNA storage buffer composition on fragmentation and library yield when using the Twist TrueAmp Library Preparation Kit. Together, these results provide practical guidance for tuning enzymatic fragmentation conditions to generate high-quality libraries tailored to specific sequencing applications.

METHODS

Libraries were prepared using the Twist TrueAmp Library Preparation Kit according to the manufacturer's protocol, with the exception of intentional perturbations to fragmentation duration and SPRI bead purification ratios. For all experiments, 50 ng of genomic DNA from the Coriell NA12878 reference sample was used as input. During library construction, 5 µl of Twist Universal Adapters were used for ligation, and 10 µl of Twist Unique Dual Indexed (UDI) primers were used for PCR amplification. Amplification was performed using the Twist TrueAmp Polymerase Mix. SPRI bead-based purification was carried out using Twist SPRI purification beads.

Library quality was evaluated using two orthogonal methods. Library yield was quantified using the Qubit dsDNA Broad Range Assay (Thermo Fisher Scientific) and calculated as the measured concentration multiplied by a final elution volume of 20 µl. Fragment size distributions were assessed using the D1000 ScreenTape Assay on the Agilent TapeStation. Sequencing was performed on an Illumina NextSeq 550 platform using a high-output kit, generating 2 × 74 bp paired-end reads. Reads were aligned to the reference genome using BWA, and library metrics including insert size and GC uniformity were calculated using Picard tools.

RESULTS

INSERT SIZE CAN BE OPTIMIZED WITH TIME & TEMPERATURE

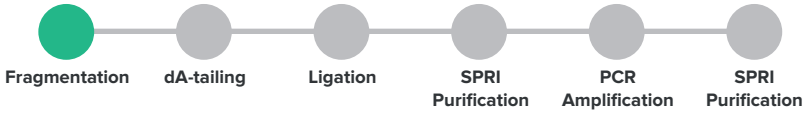

Enzymatic fragmentation enables precise modulation of DNA fragment size through adjustment of reaction parameters. To evaluate this, genomic DNA was fragmented across a range of temperatures and incubation times relative to the standard condition (32°C, 22 min), followed by a fixed 65°C incubation for dA-tailing.

Fragment size distributions were assessed following library preparation using TapeStation analysis (**Figure 1**). A gel representation of fragment size distributions across conditions demonstrates that both temperature and incubation time serve as effective tuning parameters. Increasing either parameter resulted in progressively shorter fragment sizes, consistent with increased nuclease activity. Conversely, lower temperatures or shorter incubation times preserved longer fragments, though often with broader size distributions.

A.

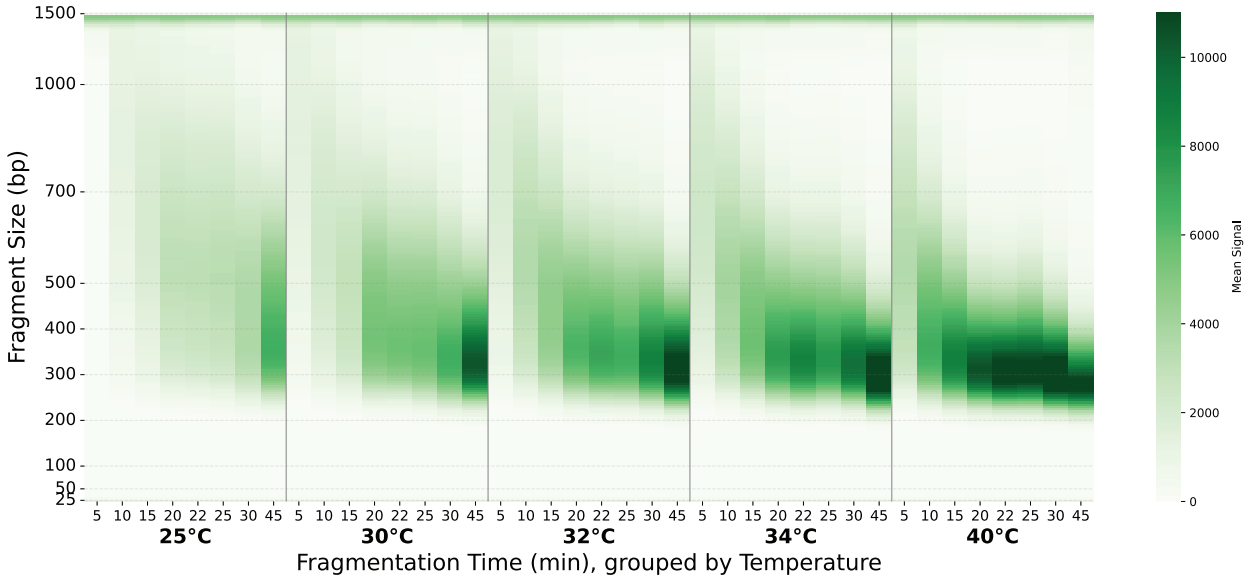

B.

	AVERAGE TAPESTATION SIZE (BP)				
	25°C	30°C	32°C	34°C	40°C
5 min	750	627	607	586	540
10 min	628	568	547	520	449
15 min	586	520	496	468	403
20 min	549	476	446	421	366
22 min	537	461	430	403	360
25 min	530	452	420	410	361
30 min	494	420	408	385	340
45 min	456	390	365	342	316

Figure 1. (A) Gel representation of DNA fragment size distributions and (B) table depicting average TapeStation size across fragmentation temperatures and incubation times. Genomic DNA was enzymatically fragmented under varying conditions (25–40°C, 5–45 minutes), and fragment size distributions were assessed by TapeStation analysis after ligation and PCR. Average library sizes calculated from TapeStation analysis between 100–1000 bp are shown for all conditions tested. Signal intensity (green) reflects relative abundance of fragments at each size. Conditions are grouped by temperature (25–40°C), with increasing incubation time shown within each group. Increasing fragmentation time and temperature result in a progressive shift toward smaller fragment sizes and enrichment of final libraries in the ~200–400 bp range. Peaks corresponding to internal size standards are visible at ~25 bp and ~1500 bp.

These results demonstrate that fragmentation time and temperature act as interchangeable adjustment parameters, enabling similar fragment size distributions to be achieved through different combinations of conditions (**Figure 2**). For example, extended incubation at a moderate temperature (e.g., 32°C at 45 mins) can produce fragment sizes comparable to those generated at higher temperatures with shorter incubation times (e.g., 40°C at 20 mins). This flexibility allows users to select conditions based on their desired insert size while balancing workflow constraints such as reaction time and the need to preserve longer DNA fragments.

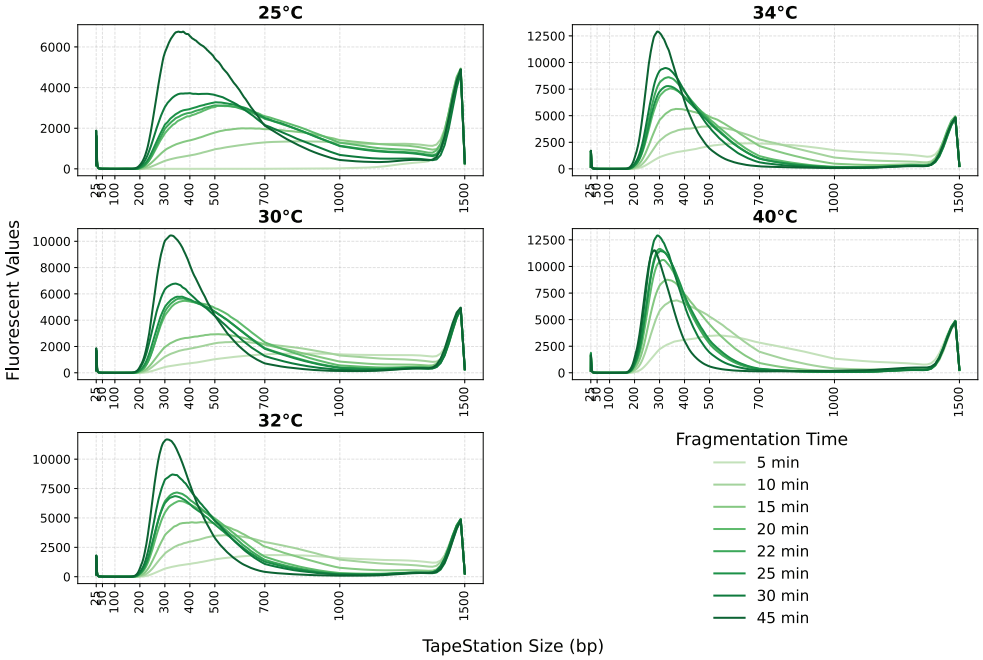

Figure 2. Electropherogram traces of DNA fragment size distributions across fragmentation temperatures and incubation times. Each panel represents a single temperature, with color intensity corresponding to incubation time. Increasing fragmentation time results in a progressive shift toward smaller fragment sizes and increased peak intensity in the ~200–400 bp range. Higher temperatures accelerate this shift, producing narrower and more concentrated fragment distributions. Internal size standards are visible at ~25 bp and ~1500 bp across all conditions.

FRAGMENTATION CONDITIONS INFLUENCE INSERT SIZE AND LIBRARY YIELD

Following the demonstration that insert size can be tuned through fragmentation time and temperature, we next evaluated how these parameters influence overall library yield. Across all conditions tested, a clear inverse relationship was observed between fragment size and library yield, with smaller fragments consistently producing higher yields. Exact post-PCR yields are shown in (**Table 1**), where 50 ng of genomic DNA was used as input. This trend is also captured in (**Figure 3**), where the strong linear correlation (R^2 = 0.904) highlights the tradeoff between maintaining larger insert sizes and maximizing library conversion efficiency.

This relationship provides a practical framework for optimization, allowing users to select conditions based on both target insert size and yield requirements. For applications prioritizing sensitivity or input recovery, smaller fragment sizes and higher yields may be preferred, while workflows requiring greater genomic context may benefit from preserving larger inserts. However, milder fragmentation conditions that generate larger fragments may also result in incomplete fragmentation, producing longer DNA molecules that are less efficiently amplified under standard PCR conditions. In these cases, increasing input DNA mass can help compensate for reduced amplification efficiency and ensure sufficient library yield.

Together, these results demonstrate that fragmentation conditions can be systematically tuned to control both fragment size distribution and library yield. Lower temperature or shorter incubation conditions favor larger inserts (~500–600 bp), which can improve mapping performance, reduce edge effects, and minimize read overlap in paired-end sequencing, while higher temperature or longer incubation conditions generate smaller fragments (~300–400 bp) with increased library yield due to more efficient enzymatic processing and amplification. This tunability enables selection of conditions based on the specific requirements of downstream sequencing applications.

TEMPERATURE (°C)	DURATION (MINUTES)	AVERAGE TAPESTATION SIZE (BP)	LIBRARY YIELD (NG)
25	5	750	30
25	10	628	1220
25	15	586	1440
25	20	549	1940
25	22	537	2070
25	25	530	1960
25	30	494	2240
25	45	456	2510
30	5	627	1000
30	10	568	1750
30	15	520	1940
30	20	476	2550
30	22	461	2390
30	25	452	2500
30	30	420	2700
30	45	390	2900
32	5	607	1300
32	10	547	1900
32	15	496	2330
32	20	446	2850
32	22	430	2740
32	25	420	2800
32	30	408	3030
32	45	365	3020
34	5	586	1500
34	10	520	2000
34	15	468	2480
34	20	421	2990
34	22	403	2900
34	25	410	2780
34	30	385	2810
34	45	342	3120
40	5	540	2000
40	10	449	2700
40	15	403	2900
40	20	366	2900
40	22	360	3100
40	25	361	3200
40	30	340	3200
40	45	316	3300

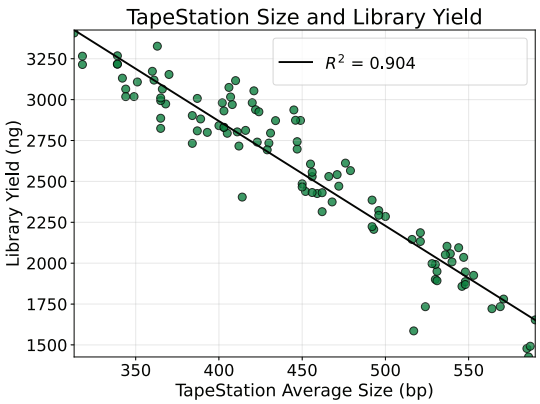

Figure 3. Relationship between NGS DNA library size and library yield. Each point represents an individual fragmentation condition across temperatures and incubation times. A strong inverse correlation is observed (R^2 = 0.904), indicating that smaller fragment sizes are associated with higher library yields. This relationship reflects increased enzymatic processing efficiency under more stringent fragmentation conditions, resulting in greater conversion of input DNA into sequencing-ready libraries.

Table 1. Summary of DNA fragment size and library yield across enzymatic fragmentation conditions. Genomic DNA was fragmented over a range of temperatures (25–40°C) and incubation times (5–45 min). Average fragment size was determined by TapeStation analysis between 100–1000 bp and library yield was measured by Qubit Broad Range dsDNA assay post-library prep. Values represent mean ± standard deviation from triplicate reactions.

CONTROL OF INSERT SIZE & YIELD THROUGH SPRI SIZE SELECTION

While enzymatic fragmentation establishes the initial DNA fragment size distribution, SPRI-based purification provides a secondary tuning lever to further refine library insert size. By adjusting the SPRI bead-to-sample ratio, users can selectively retain or exclude DNA fragments based on size, enabling targeted removal of smaller fragments that fall outside the desired range. Lower SPRI ratios preferentially retain larger DNA fragments, resulting in a right-shifted size distribution, while higher ratios increasingly retain shorter fragments.

Importantly, SPRI-based size selection can be applied at multiple stages of the workflow, including both pre- and post-PCR, providing flexibility in shaping the final library profile. Pre-PCR SPRI allows refinement of the input fragment pool prior to amplification (**Figure 4**), while post-PCR SPRI further sharpens the final library distribution (**Figure 5**). Together, these results demonstrate that SPRI ratio can be used in conjunction with fragmentation conditions to precisely tune library insert size, enabling optimization of both fragment distribution and downstream sequencing performance.

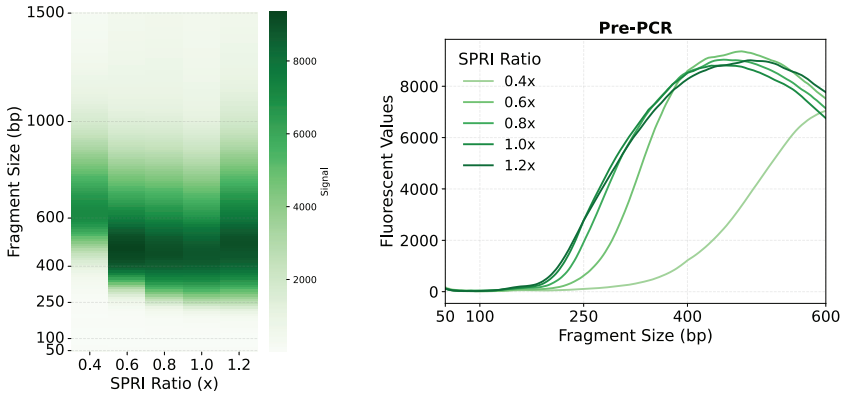

Figure 4. Effect of pre-PCR SPRI ratio on library size distribution. Libraries were subjected to SPRI purification following ligation using bead-to-sample ratios ranging from 0.4× to 1.2×. Gel representation (left) and representative TapeStation electropherograms (right) demonstrate that decreasing SPRI ratio selectively removes shorter DNA fragments, resulting in enrichment of larger DNA fragments, while reducing overall library complexity due to loss of smaller molecules.

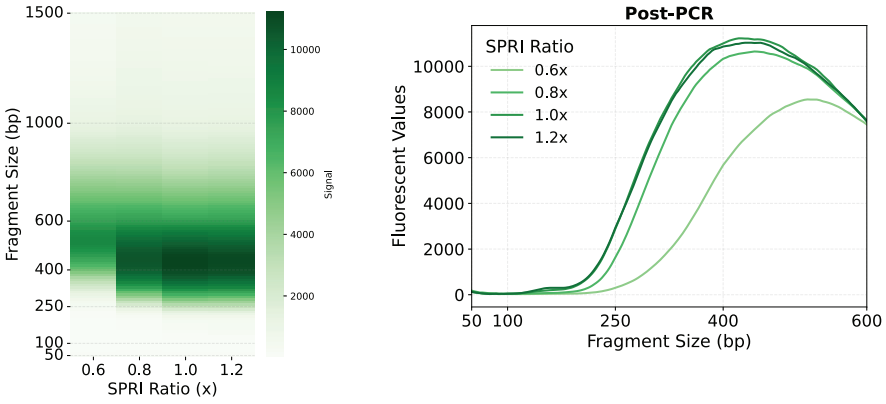

Figure 5. Effect of post-PCR SPRI ratio on final library size distribution. Following PCR amplification, libraries were subjected to SPRI purification using bead-to-sample ratios ranging from 0.6× to 1.2×. Gel representation (left) and representative TapeStation traces (right) demonstrate similar effect as pre-PCR SPRI where decreasing ratios selectively removes shorter DNA fragments.

RELATIONSHIP BETWEEN LIBRARY SIZE AND SEQUENCED INSERT SIZE

To assess how library size measured by TapeStation translates to sequencing insert size, libraries generated under varying fragmentation conditions were sequenced on the Illumina NextSeq 550 platform. While TapeStation provides an estimate of fragment size distribution, the effective insert size observed during sequencing can differ due to factors such as adapter contribution, size selection biases, and preferential amplification of certain fragment lengths.

Our results demonstrate that sequencing-derived insert sizes are consistently smaller than TapeStation-derived library sizes, with a systematic offset that can be partially explained by adapter contribution (~140 bp). However, the observed insert sizes fall below this adapter-corrected expectation, particularly at larger fragment sizes, indicating an additional bias during sequencing (**Figure 6**).

This systematic deviation highlights that longer DNA fragments are underrepresented during sequencing, likely due to reduced clustering efficiency on the Illumina flow cell. As a result, TapeStation measurements should be interpreted as an upper-bound estimate of effective sequencing insert size. This effect becomes increasingly pronounced at larger fragment sizes and should be considered when optimizing library preparation conditions for applications requiring precise insert size control.

To further evaluate whether insert size influences sequencing performance beyond clustering efficiency, we examined GC bias across libraries spanning a range of insert sizes. Normalized coverage profiles are highly consistent across GC content bins for all insert sizes evaluated (**Figure 7**). Minimal divergence is observed across most of the GC spectrum, with only modest variability at extreme GC content (<10% and >80%), consistent with known sequencing and amplification biases. Notably, no systematic shift in GC bias is observed with increasing insert size, indicating that GC uniformity is largely independent of fragment length within the tested range. These results suggest that insert size optimization can be performed to balance clustering efficiency and desired fragment length without introducing additional GC-related coverage bias.

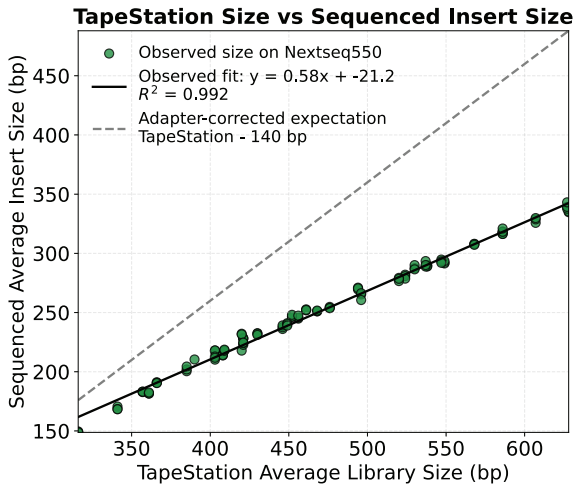

Figure 6. TapeStation library size versus sequenced insert size. Measured insert sizes from NextSeq 550 sequencing are plotted against TapeStation-derived library sizes. The dashed line represents the expected insert size after subtracting the adapter contribution (~140 bp), while the solid line indicates the observed linear fit (R^2 = 0.922). Sequenced insert sizes are consistently lower than expected, with increasing deviation at larger fragment sizes, consistent with reduced clustering efficiency of longer DNA fragments.

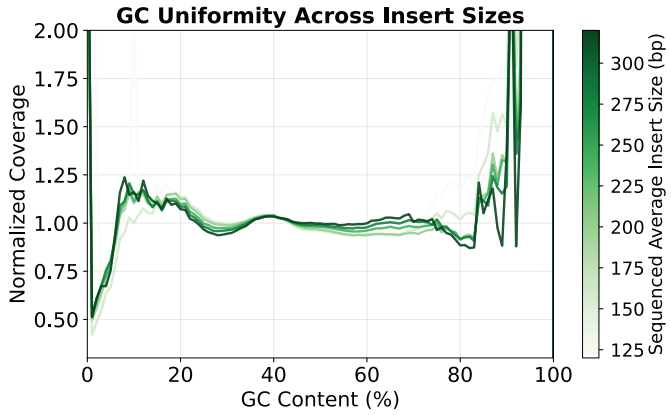

Figure 7. GC uniformity across sequenced insert sizes. Normalized coverage is plotted as a function of GC content for libraries spanning a range of insert sizes (color gradient, lighter to darker green indicating increasing insert size). Coverage was normalized within each library to highlight GC-dependent bias independent of overall yield. Across the evaluated insert size range (~120–320 bp), GC bias profiles are highly similar, with minimal divergence observed across most GC content bins. Slight variability is observed at extreme GC content (<10% and >80%), consistent with known sequencing and amplification biases.

IMPACT OF DNA STORAGE BUFFER ON FRAGMENTATION AND INSERT SIZE CONTROL

While fragmentation conditions and SPRI-based size selection provide robust control over library insert size, upstream sample composition represents an important and often overlooked variable. In particular, the storage buffer of input DNA can significantly influence enzymatic fragmentation efficiency, leading to deviations from expected insert size distributions.

To systematically evaluate this effect, common buffer components—including salts, chelating agents, and detergents—were introduced across a range of concentrations. Increasing concentrations of NaCl, EDTA, and SDS result in clear, dose-dependent shifts in insert size and library yield (**Figure 8**). In general, inhibition of fragmentation manifests as an increase in apparent insert size, consistent with reduced nuclease activity. This effect is often accompanied by a reduction in library yield, reflecting impaired enzymatic processing and downstream conversion efficiency.

Mechanistically, these effects are consistent with known biochemical interactions: EDTA chelates divalent cations required for nuclease activity, salts modulate enzyme–DNA interactions, and detergents such as SDS can directly disrupt protein structure. Notably, these effects are not always linear—some components exhibit gradual inhibition, while others produce sharp failure thresholds where library generation is severely compromised.

Importantly, partial recovery of fragmentation performance can be achieved through buffer modulation. The addition of NP-40 can mitigate SDS-mediated inhibition, restoring both insert size distribution and library yield across a range of conditions (**Figure 9**). This highlights that fragmentation efficiency is not solely dictated by time and temperature of enzymatic reactions, but is highly sensitive to the surrounding chemical environment.

Together, these results demonstrate that DNA storage buffer composition can substantially impact both fragmentation behavior and overall library performance. For optimal reproducibility, DNA input should be prepared in low-salt conditions (e.g., nuclease-free water or low-EDTA buffers). However, when inhibitory components are present, fragmentation conditions can often be adjusted to compensate. In particular, extending fragmentation time or increasing temperature can help overcome partial inhibition, as the trends described above provide a useful framework for identifying conditions that recover the desired insert size.

In cases where performance remains inconsistent or significantly impaired, users should consider purifying the input DNA to remove potential inhibitors and confirm whether buffer composition is the underlying cause. This approach can help distinguish between sample-related effects and intrinsic limitations of the fragmentation workflow, enabling more targeted optimization.

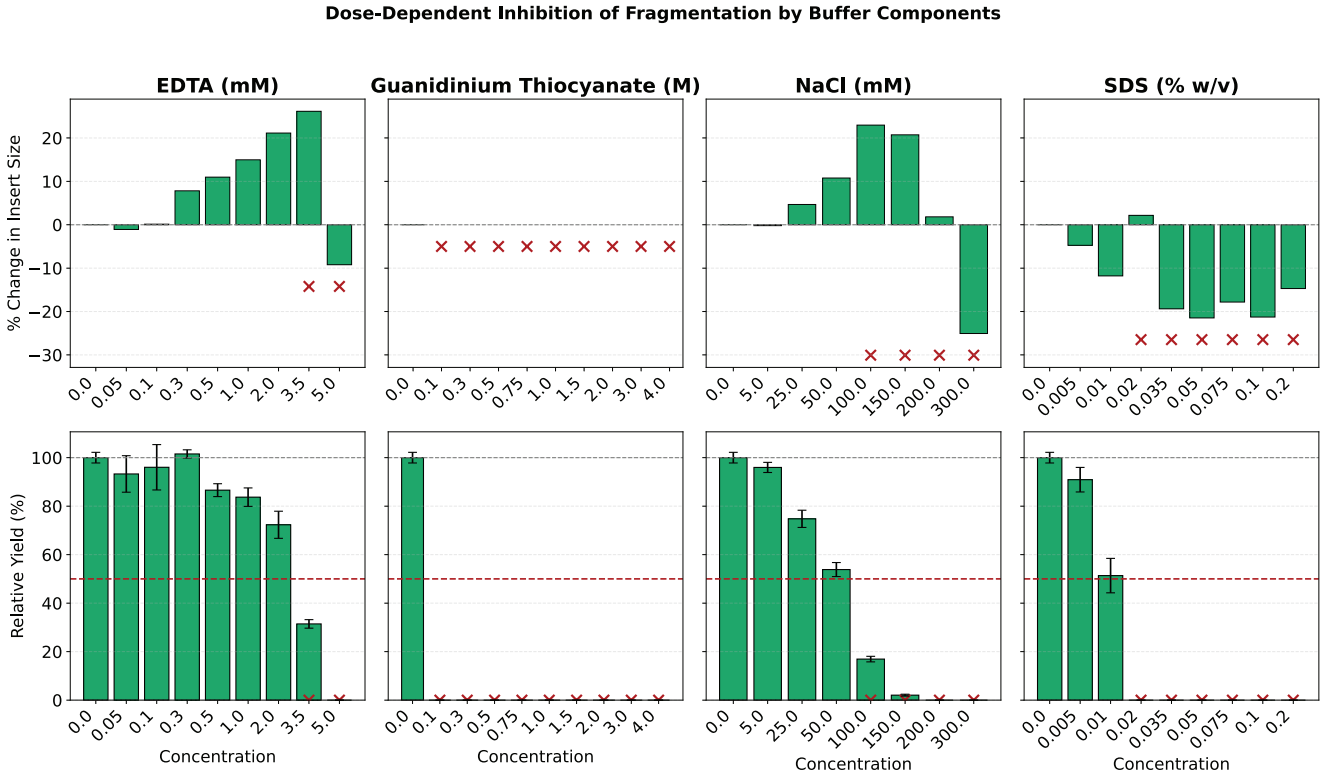

Figure 8. Dose-dependent inhibition of enzymatic fragmentation by common buffer components. Genomic DNA was fragmented in the presence of increasing concentrations of EDTA, guanidinium thiocyanate, NaCl, and SDS. Insert size is represented as percent change relative to control conditions (top), and library yield is shown as relative yield normalized to control by buffer component concentration (bottom). Increasing concentrations of inhibitory components result in a shift toward larger insert sizes, consistent with reduced fragmentation efficiency, accompanied by a decrease in library yield. Red "X" markers indicate conditions where library yield falls below 50% or where library generation fails entirely. Concentrations of components are calculated as the final concentration in the fragmentation reaction of 50 µl.

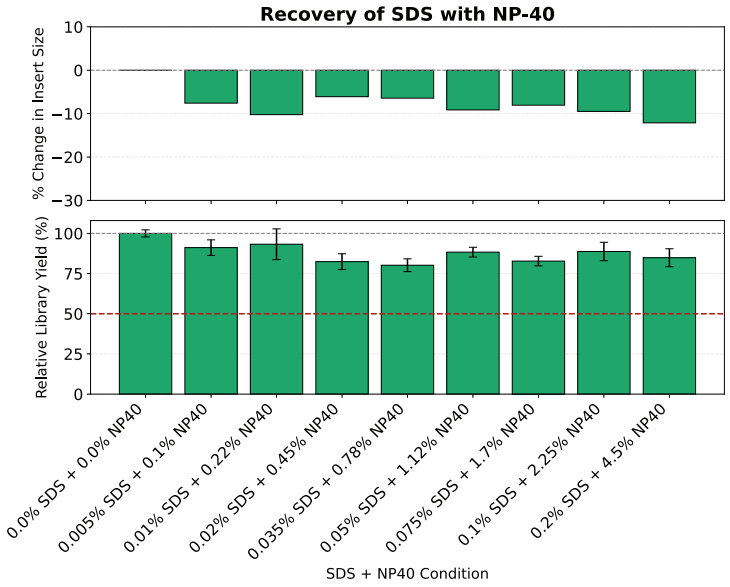

Figure 9. Recovery of SDS-mediated inhibition through NP-40 supplementation. Fragmentation reactions were performed in the presence of SDS with increasing concentrations of NP-40. Insert size (top) and library yield (bottom) are shown relative to control conditions. SDS alone reduces fragmentation efficiency and library yield, resulting in larger apparent insert sizes. Addition of NP-40 partially restores both insert size distribution and library yield across a range of conditions, indicating that detergent-mediated inhibition can be mitigated through additives.

CONCLUSION

Enzymatic fragmentation within the Twist TrueAmp workflow provides a flexible and tunable approach for controlling DNA fragment size and optimizing sequencing performance. Fragmentation time and temperature act as interchangeable adjustment parameters to modulate insert size, while SPRI-based size selection offers a secondary mechanism to further refine library distributions.

Sequencing analysis shows that effective insert sizes are consistently smaller than TapeStation estimates, particularly for larger fragments, due to clustering biases. Importantly, GC uniformity remains largely unaffected across the tested insert size range, allowing insert size to be optimized independently of GC bias.

Finally, DNA storage buffer composition can significantly impact fragmentation performance. Common buffer components may inhibit enzymatic activity, resulting in larger insert sizes and reduced yield. While mild inhibition can often be addressed by adjusting fragmentation conditions, more severe effects may require sample purification.

Together, these results provide a practical framework for tuning fragmentation conditions, refining library profiles, and achieving consistent, high-quality performance across a wide range of sequencing applications